Research on distortion quality evaluation of computer network shared image based on visual sensitivity

Junru Li

School of Information Engineering,
Xinyang Agriculture and Forestry University,
Xinyang City, Henan Province, China
Email: lijunru5921@126.com

Abstract: Shared image distortion will affect the user's experience, and then damage people's life and entertainment experience. In view of this, this research starts with the evaluation and classification of network shared image distortion quality, improves the shared image distortion quality evaluation algorithm combined with the sensitive characteristics of human vision, and verifies its performance superiority through comparative experiments. The results show that the performance of some improved reference quality evaluation algorithms reaches the highest values, which are 0.7923, 0.3224, 0.7931 and 0.8213, respectively. The improved non-reference quality evaluation algorithm achieves the highest values of positive indicators in the comparison of performance values, which are 0.487 and 0.287, respectively, while the lowest value of negative indicators is 0.902. It can be seen that the improved shared image quality evaluation algorithm conforms to the sensitive characteristics of human eyes, has high computational efficiency and has broad application prospects.

Keywords: image quality evaluation; visual sensitivity; partial reference evaluation; no reference evaluation.

Reference to this paper should be made as follows: Li, J. (2023) 'Research on distortion quality evaluation of computer network shared image based on visual sensitivity', *Int. J. Wireless and Mobile Computing*, Vol. 24, No. 1, pp.27–37.

Biographical notes: Junru Li received Master degree and she is a Lecturer in Xinyang Agriculture and Forestry College. Her research interests include cloud computing and computer networks. She has been engaged in the research and teaching of Computer Application Technology for a long time. In recent years, she has participated in the compilation of one textbook and won the first prize of Xinyang Excellent Paper Achievement. Besides, two utility model patents, six software Copyrights and 16 related professional papers were published, including one paper in EI Journals and another in Chinese core journals.

1 Introduction

With the development of social digitisation and informatisation, computer network shared images have been fully used in life. The sharing and real-time communication of visual information provide more convenient ways of work and entertainment for people who can't communicate face-to-face. Accordingly, the image loss caused by image compression and transmission in the process of network sharing has caused many adverse effects on the user experience. Therefore, the evaluation method of shared image distortion quality in computer network has become an important topic in related fields (Aich et al., 2020; Song et al., 2019; Wang et al., 2019a). Since the final receiver of network shared images is human vision, the sensitive features of human vision system for images have a crucial impact on image quality evaluation in the process of image quality evaluation (Akb et al., 2019; Fang et al., 2021; Qu et al., 2021). Therefore, starting with the sensitive characteristics of human visual system, evaluating the distortion quality of computer network shared pictures through intelligent algorithms, and then helping to improve the quality of network shared pictures is one of the important directions of future development. The perfect and efficient network shared picture distortion quality evaluation system can not only quickly reflect the real quality of the picture, but also make a quantitative output measurement for the output of the codec, ensure the service quality to users, and help to design and optimise the display system in line with the sensitive characteristics of human vision (Chen et al., 2021; Zhaolin et al., 2021; Bouida et al., 2021).

At present, the research on computer vision and image is gradually deepening, and the application fields are gradually increasing. Based on the deep learning network, Yang and Song (2022) designed a new central loss function by using the structure of migration learning algorithm to mark the face image data under different light intensities in the field environment. The results show that this loss function can improve the accuracy of face recognition under different light intensities, reaching 99.65%; Lei (2022) designed an improved algorithm combining the target detection technology. The algorithm combines the Gabor wavelet transform algorithm with the principal component analysis algorithm. It has a significant effect on character recognition in video. The results show that the recognition accuracy of the designed algorithm is 86.34%, while the recognition time is only 34.28 s, which is higher than the accuracy and efficiency of the traditional algorithm (Lei, 2022); Wang et al. (2019b) proposed a non-reference image quality evaluation method based on convolutional neural network and focusing on the significance of local images. The test results show that the evaluation index of this method is obviously due to the traditional two-dimensional image quality evaluation index (Wang et al., 2019b); Xiao et al. (2021) proposed an image interpolation method based on wavelet domain optimal transmission technology, which can be compatible with any network structure and parameter requirements. The research results show that compared with the existing single image super-resolution method, this method can achieve a balance between the distortion effect of super-resolution and food quality (Xiao et al., 2021). The research on the establishment of the distortion quality evaluation system for computer network shared images is conducive to the accurate quantitative evaluation of image quality in image sharing, help designers and inspectors find out the quality defects in shared images and then promote the improvement of network shared image quality.

2 Research on distortion quality evaluation system of computer network shared image based on visual sensitivity

2.1 Partial reference quality evaluation system for network shared image quality

In the network shared image, the image quality is often extremely important. The image distortion caused by network compression often significantly affects the user experience. At present, there are mainly two methods for image quality evaluation, namely subjective image quality evaluation and objective image quality evaluation. Subjective image quality evaluation takes the subjective perceived opinion value as the real-value of distorted image quality, and uses it to test and optimise the algorithm. At present, there is a screen image quality assessment data set Screen Image Quality Assessment Database (SIQAD) to obtain subjective scores through 11 absolute categories proposed by the International Telecommunication Union (Ng et al., 2020). However, the subjectivity of this method is still very strong, so this study adopts the objective image quality evaluation method. Objective image quality evaluation simulates the human eye by establishing a model following human visual characteristics, and then evaluates the image distortion quality (Ng et al., 2020). Objective image quality evaluation is divided into full reference image quality evaluation Full Reference (FR), partial reference image quality evaluation Reduced Reference (RR) and no reference image quality evaluation No Reference (NR) (Meng et al., 2020). The full reference image quality evaluation needs complete reference information to evaluate the image distortion quality by measuring the difference between the reference image and the distorted image. This method is demanding, and it is often difficult to obtain all the information of the original image in practical application. Therefore, the comparison of some reference images and no reference images is more practical. Partial reference image quality evaluation can compare the reference image with the distorted image when only partial reference image information is extracted, as shown in Figure 1.

Some existing reference image quality models try to reduce the amount of reference information required while ensuring accurate predictability. The following sampling methods and methods based on statistical model parameters try to make the model more efficient from this point of view. Since the essence of image distortion quality evaluation is based on the different effects observed and recognised by the shared receiver, this study will propose a partial reference quality algorithm based on visual sensitivity and network shared image information content from another perspective, that is, human visual sensitivity. The algorithm extracts the visual sensitivity and information content feature map based on the reference image and the distorted image, respectively, and then obtains the corresponding feature vector and finally obtains the quality evaluation score. See Figure 2 for details.

Figure 1 Partial reference image quality evaluation framework

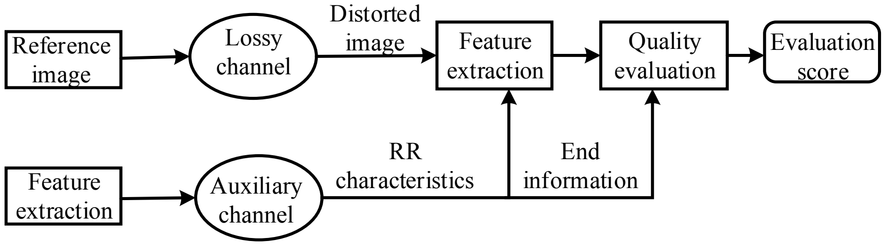

Figure 2 Partial reference image quality evaluation algorithm flow

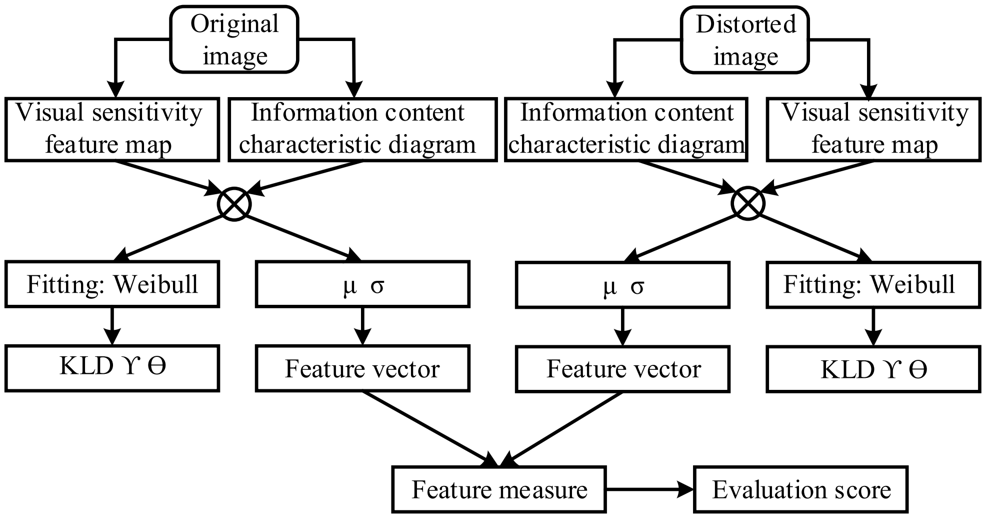

As shown in Figure 2, the process of obtaining feature vectors from feature maps focuses on feature extraction. In image content, features often include image colour, image texture, image edge, etc. since image edge has been widely used as an important index for image content evaluation, this research will also take image edge information as the main expression of image features and select ScHARR operator that can establish statistical model for edge extraction. The formula is as follows:

$$g_x = H \otimes x = \begin{bmatrix} +3 & 0 & -3 \\ +10 & 0 & -10 \\ +3 & 0 & -3 \end{bmatrix} \otimes x \tag{1}$$

$$g_y = V \otimes x = \begin{bmatrix} +3 & +10 & +3 \\ 0 & 0 & 0 \\ -3 & -10 & -3 \end{bmatrix} \otimes x \tag{2}$$

where H represents the filter in the horizontal direction of Scharr and V represents the filter in the vertical direction of Scharr. The corresponding gradient amplitude is calculated as follows:

$$GM = \sqrt{g_x^2 + g_y^2} \tag{3}$$

Since the human visual system is more sensitive to the compression distortion of the flat area in the network shared image than the texture area, the visual sensitivity is defined as the amplitude difference between adjacent pixels in the image. The visual sensitivity formula is as follows:

$$S(i,j) = \left| P(i,j) - \hat{p}(i,j) \right| \tag{4}$$

where $P(i,j)$ represents the actual value of point (i,j), and $\hat{p}(i,j)$ represents the predicted value of (i,j) point at the current position. Since the amplitude of any pixel in the image can be expressed in the form of the sum of the weighted average of pixels in its adjacent area and noise, $\hat{p}(i,j)$ can be calculated as:

$$\hat{p}(i,j) = WX(i,j) \tag{5}$$

$$W = C_{PX} C_X^{-1} \tag{6}$$

$$C_{PX} = E\left[PX^T\right] \tag{7}$$

$$C_X = E\left[XX^T\right] \tag{8}$$

where X is the vector matrix composed of the neighbourhood vector of each point to be predicted, $X(i,j)$ is the vector composed of pixels in the adjacent area of the point (i,j), C_{PX} is the covariance between P and X, and the distribution diagram of points in the neighbourhood is shown in Figure 3.

Figure 3 Distribution of neighbourhood points

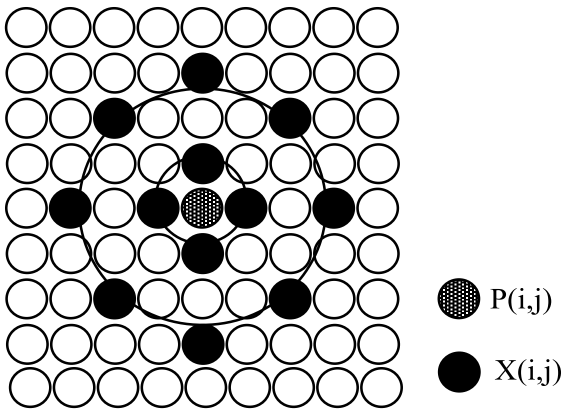

As shown in Figure 3, the light colour points are $P(i,j)$, the surrounding dark points are neighbourhood points $x(i,j)$ and the neighbourhood vector $X(i,j)$ is composed of all dark points. Since the difference between the predicted value $\hat{p}(i,j)$ and the actual value $P(i,j)$ is the visual sensitivity, it is only necessary to traverse all (i,j) to characterise the sensitivity as a whole. Because the sensitivity of human vision to text area is higher than that of image area, the established model should not only simulate the sensitivity of human vision to text area, but also simulate the slightly weak sensitivity of human vision to image area. However, this effect is difficult to achieve only by relying on the pixel level visual sensitivity map. Therefore, it is necessary to fuse the pixel level and edge features level sensitivity to obtain the final sensitivity map, so as to achieve a balanced effect on the phase sensitivity simulation. It is worth not that the final feature map is obtained by multiplying the gradient amplitude map representing the image content and the visual sensitivity map. This method often requires a large amount of information about the calculation process. In order to optimise the calculation efficiency, the parameters of the statistical model are used as reference information to reduce the amount of data, which is approximately expressed by the Weibull distribution of the statistical model, and the formula is:

$$f(x) = \left(\frac{\gamma}{\theta}\right) x^{\gamma-1} \exp\left(-\frac{x^{\gamma}}{\theta}\right) \tag{9}$$

where γ represents the shape parameter and θ represents the distribution scale parameter. The reference information formula can be expressed as:

$$f_r = f_d = \{\mu, \sigma, \gamma, \theta, KLD\} \tag{10}$$

where μ represents the mean value of characteristic graph coefficients, θ represents the variance of characteristic graph coefficients, γ and θ are the parameters of statistical model Weibull and KLD is used to measure the fitting accuracy of Weibull. Finally, based on the non-linear fusion of the reference image and the distorted image, the evaluation quality score is:

$$SIQA = \frac{1}{N}\sum_{i=1}^{N}\left(1 - \frac{|f_r(i) - f_d(i)|}{f_r(i) + f_d(i) + \varepsilon}\right) \tag{11}$$

where N refers to the number of reference information, and ε refers to a constant whose denominator is not 0. This value is generally small, usually 0.001.Since this constant is used to avoid converting the denominator to the value of 0, the constant unit that will not affect the accuracy is generally used when determining this value, which is usually 0.001.

2.2 No reference quality evaluation system for network shared image quality

In addition to some reference quality evaluation, non-reference images quality evaluation is also an important part of objective image quality evaluation. Non-reference images quality evaluation does not need any information about the reference image, but evaluates the quality based on the internal law related to the image quality. Non-reference quality evaluation is suitable for screen content video sharing with network shared images. Screen content video is essentially an image sequence composed of a series of images that change from time of the computer screen. Compared with the conventional external landscape, screen content video is often more complex and diverse, which will stimulate human vision. Therefore, a large amount of calculation data is often involved in image quality evaluation, full reference quality and partial reference quality are not suitable. Only non-reference quality evaluation can improve the calculation efficiency. At present, the commonly used non reference quality evaluation is divided into two categories: one is the quality evaluation based on the number of frames, and the other is the quality score obtained by combining spatial features of time-domain features. In this study, the algorithm design is based on the combination of non-reference quality evaluation and visual attention features in the process of human visual viewing screen content video. See Figure 4 for details.

Figure 4 Algorithm flow chart

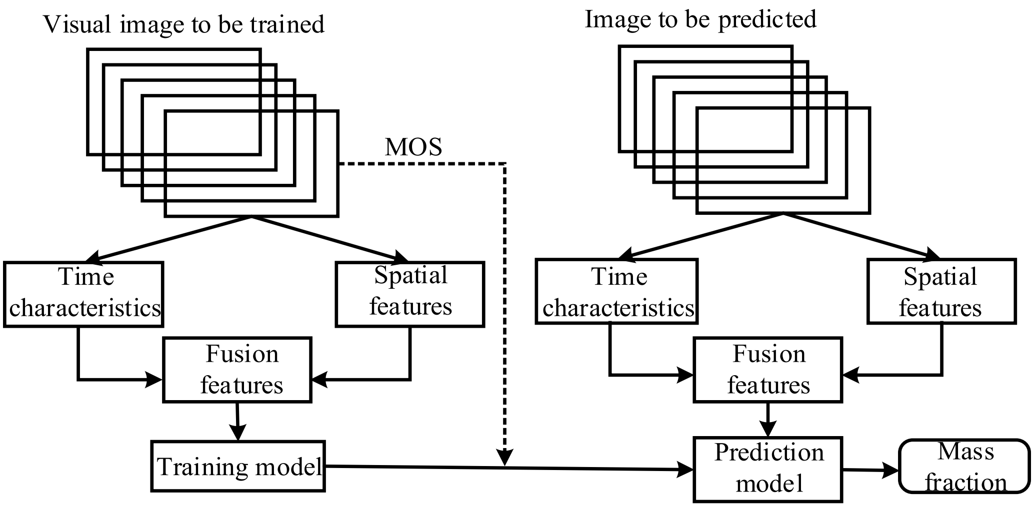

As shown in Figure 4, the algorithm divides the sample image into two parts: the image to be trained and the image block to be predicted. The two parts extract the temporal and spatial features, respectively. After extraction, the temporal and spatial features are fused to form the training model and prediction model respectively. Finally, the quality evaluation score of the network shared image is obtained through the prediction model. Before feature extraction, it is necessary to distinguish the visual significance effect of image content. The specific algorithm pseudo code is:

Algorithm input:

Training sets $I_1, I_2, ..., I_m$;

The corresponding JND images of distorted images in the training set are $J_1, J_2, ..., J_m$;

Supervisor tag values $S_1, S_2, ..., S_m$;

Training steps:

(1) Initialise network parameters, set batch size=8, epoch=50, step=m/batch size, where *M* represents the training sample capacity.

(2) Network training phase 1:

for *i*=1 to epoch;

for *j*=1 to step;

The objective mass fraction is obtained by forward calculation according to the space-time characteristics;

Calculate the error between prediction quality and subjective MOS

Freeze the parameters, update the parameters of other layers of the network through the gradient descent method, and set the learning rate parameter as L_1;

end

end

(3) Network training phase 2:

for *i*=1 to epoch;

for *j*=1 to step;

The objective mass fraction is obtained by forward calculation according to the space-time characteristics;

Calculate the error between prediction quality and subjective MOS

Freeze the parameters, update the parameters of other layers of the network through the gradient descent method, and set the learning rate parameter as L_2;

end

end

In the practical application of daily life, the human eye mainly needs to deal with three scenes of different occasions: one is to receive images about work and life, the other is to receive entertainment and leisure images, and the third is to mix the first two. These three scene values include the reception of screen single window image output and screen multi-window image output. The three different scenes will have different effects on the eye movement effect of human visual system. Firstly, the attention regions of human visual system between continuous frames of graphics have high correlation; Secondly, in the process of receiving the image, the human visual system tends to pay more attention to the moving object or the moving part of the object and the moving part of the human visual system has high sensitivity and strong resolution; Thirdly, in the process of receiving the image, the focus of human visual system will change with the change of video motion area. When the motion frequency of the object of the shared image is not high, the human visual system will focus on the relatively static part, and the observation and resolution of this part will be improved rapidly. When the object motion frequency increases, the focus on human visual system will be quickly pulled to the changing image area, so as to achieve the resolution effect of moving objects; Finally, in the process of receiving images, the focus of human visual system is often distributed in the middle, upper left, lower left and upper right areas of the screen, showing the characteristics of distribution with the area. Therefore, according to the significant concentration and resolution of the human visual system for moving objects, this study will focus on the motion of the image in the feature extraction part. At the same time, for the observation ability of the human visual system when facing the still image, it will also focus on the impact of the content of the screen image, so as to distinguish the temporal and spatial nature of the image. The extraction process of spatial features is shown in Figure 5.

Figure 5 Spatial feature extraction

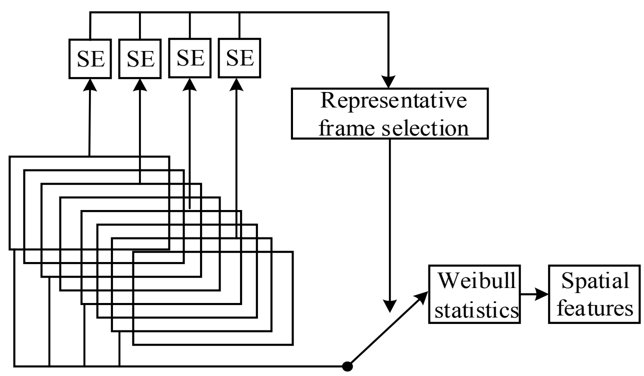

As shown in Figure 5, the extraction of spatial features is based on the extraction of statistical features of screen image content. The traditional spatial feature extraction is to extract the spatial feature of each frame image, and then calculate its mean value. This method has high calculation intensity, long time and low efficiency. Therefore, this research adopts the way of spatial feature extraction of key frames to improve the computational efficiency. The main method are to sample the food sequence of/in the interval frame, and then divide the sampled image sequence according to the time length. This division will obtain an equal time interval, and calculate the spatial entropy se (special entropy) of a single frame of these equal time intervals. The spatial entropy se can fully express the complexity of the image texture, and then reflect the amount of information contained in the image. In these single frame sets, the single frame with the largest se value are selected as the representative frame, and the spatial features are extracted according to the feature extraction method of the previous section .The statistical parameters can still be extracted by Weibull and expressed by $f_r = f_d = \{\mu, \sigma, \gamma, \theta, KLD\}$. Compared with the spatial features based on the statistics of screen image content, temporal feature extraction is based on the feature extraction of human visual sensitivity. According to the visual focus of human eyes when viewing image content, the picture is divided into two dimensions: motion continuity and motion intensity, as shown in Figure 6.

Figure 6 Time feature extraction

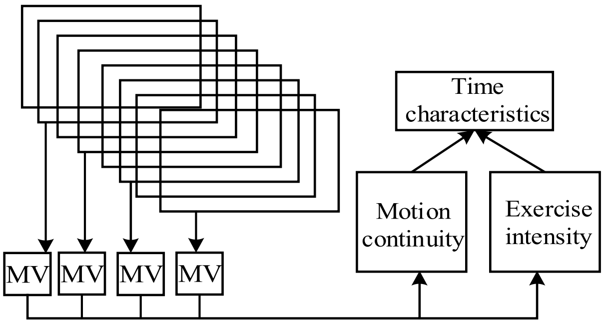

In order to reduce the computational complexity, when extracting temporal features, the image sequence is divided into equal time intervals by sampling under interval frames, the Motion Vector (MV) is estimated by motion estimation, and the motion continuity and motion intensity in each interval are further calculated, so as to complete the extraction of temporal features. In this study, the three-step search method is used to obtain the motion vector MV between two adjacent single frames. The obtained motion vector can be expressed as:

$$M(i,j) = \left[M_x(i,j), M_y(i,j)\right], i = 1,2,\ldots,L, j = 1,2,\ldots,H \quad (12)$$

L and H, respectively represent the size of the image frame, and $M_x(i,j)$ and $M_y(i,j)$, respectively represent the motion components of the position (i,j) in the horizontal and vertical directions, and the corresponding motion vector amplitude can be expressed as:

$$\|M(i,j)\| = \sqrt{M_x(i,j)^2 + M_y(i,j)^2} \quad (13)$$

At this time, except for the first frame, each single frame in each interval corresponds to a motion vector amplitude, which can be used as a basis to further calculate the motion intensity and motion continuity. Motion intensity mi (motion intensity) can be obtained by averaging the amplitudes of all motion vectors, and its formula is as follows:

$$MI(k) = \frac{\sum_{i=1}^{L}\sum_{j=1}^{H}\|M(i,j)\|}{L \times H}, k = 1,2,\ldots,N \quad (14)$$

where $MI(k)$ refers to the motion intensity of the k frame in the interval, N, represents the number of frames in the interval, L and H, respectively represent the size of each frame. The final global intensity can be calculated by using the mean value of each motion vector amplitude diagram, and the formula is as follows:

$$MI = \frac{\sum_{i=1}^{N} MI(k)}{N} \quad (15)$$

There are many methods to measure motion continuity Motion Consistency (MC). Considering the efficiency and introduction of the model, this study uses the mean square deviation of motion vector amplitude to describe motion continuity. The formula can be written as:

$$MC(k) = \sqrt{\frac{\sum_{i=1}^{L}\sum_{j=2}^{H}\left(\|M(i,j)\| - \mu\right)^2}{L \times H}}, k = 1,2,\ldots,N \quad (16)$$

where $MC(k)$ is the motion continuity of the k frame in the interval. μ is obtained by averaging the motion vector amplitude diagram of the k frame. N represents the number of frames used to divide different intervals, L and H represent the size of each frame, respectively. Finally, the global motion continuity in the interval can be expressed by the formula:

$$MC = \frac{\sum_{i=1}^{N} MC(k)}{N} \quad (17)$$

Based on the temporal and spatial features obtained above, the superposition is equivalent to that there are 5 spatial features and 2 temporal features in each interval, then the formula can be expressed as:

$$f = (\mu, \sigma, \gamma, \theta, KLD, MI, MC) \quad (18)$$

μ, σ, γ, θ and KLD are statistical parameters obtained by Weibull, while MC and MI are motion continuity and motion intensity, respectively. Finally, each interval is averaged based on the corresponding features, and then the feature vector is formed to obtain the prediction model.

3 Experimental results and analysis of distortion quality evaluation of computer network shared image based on visual sensitivity

3.1 *experimental results and analysis of partial reference quality evaluation for network shared image quality*

The experimental results and analysis of the quality evaluation of network shared image quality are divided into two parts. The first part of the experiment is the partial reference quality evaluation for the quality of network shared image, and the second part of the experiment is the non-reference quality evaluation for the quality of network shared image. Among them, some reference quality evaluation for network shared image quality will be divided into two parts: statistical parameter trend change and performance index comparison. In the part of reference quality evaluation, Screen Image Quality Assessment Database (SIQAD), Science City Database (SCD) and Instantaneous Media Laboratory-Screen Content Image Quality Database (IML-SCIQD) are used in the research. Among them, SIQAD database contains 20 original pictures and 980 corresponding distorted pictures; The SCD database contains 24 reference pictures and corresponding 492 compressed pictures, and the IML-SCIQD database contains 25 reference pictures and corresponding 1250 compressed pictures. The trend change part of statistical parameters is shown in Figure 7.

As shown in Figure 7, the JPEG compressed image and jp2k compressed image in the process of network sharing transmission are analysed this time. It can be seen that after the distortion elements are introduced into the reference image, the reference image itself begins to change with the change of distortion degree. Under this trend, the change trend of broken lines of jp2k and JPEG compressed images is basically similar, and both of them gradually decrease with the increase of distortion level. In terms of statistical parameters, the broken line height of JPEG compressed image is lower in the first and middle stages, and the downward trend is faster. However, after the distortion level exceeds level 6, the broken line of jp2k compressed image drops below the broken line of JPEG compressed image and its speed is undoubtedly faster during this period. In terms of statistical parameters, the polyline of jp2k compressed image is always below the JPEG compressed image, and the decline speed of the two polylines is similar. There is a short interleaving when the distortion level reaches level 6, which proves that the visual sensory quality of the two images is exactly the same at this time. It can be seen that when the distortion degree increases, the quality of visual perception decreases. For two different distortion types, jp2k and JPEG, although the distortion level will be slightly different, the quality of visual perception is similar. According to the fitting curves of the three images, Weibull's fitting effect is good. This way of constructing feature map is indeed helpful to provide a small amount of information for the statistical model, with high efficiency. In the performance index comparison part, this study will use PLCC index and SRCC index for performance evaluation. PLCC index evaluates the prediction accuracy by performing the nonlinear mapping between subjective and objective scores. The better the algorithm performance, the higher the PLCC value. The SRCC index is used to evaluate the monotonicity of prediction. Similarly, the better the algorithm performance, the higher the SRCC value. In the experiment, JPEG and jp2k image distortion types are also used for comparison, and three algorithms belonging to partial reference quality evaluation are selected for comparison, WNISM (WNISM method is to model the distribution of rotatable pyramid coefficients through generalised Gaussian density function, and estimate the distribution parameters as image features), DNT (Partition Normalisation Transform), EPM (Edge Pattern Model), FTD (Algorithm based on two-dimensional discrete Fourier transform) and the improved algorithm. See Figure 8 for details.

Figure 7 Correlation between statistical parameters and distortion level

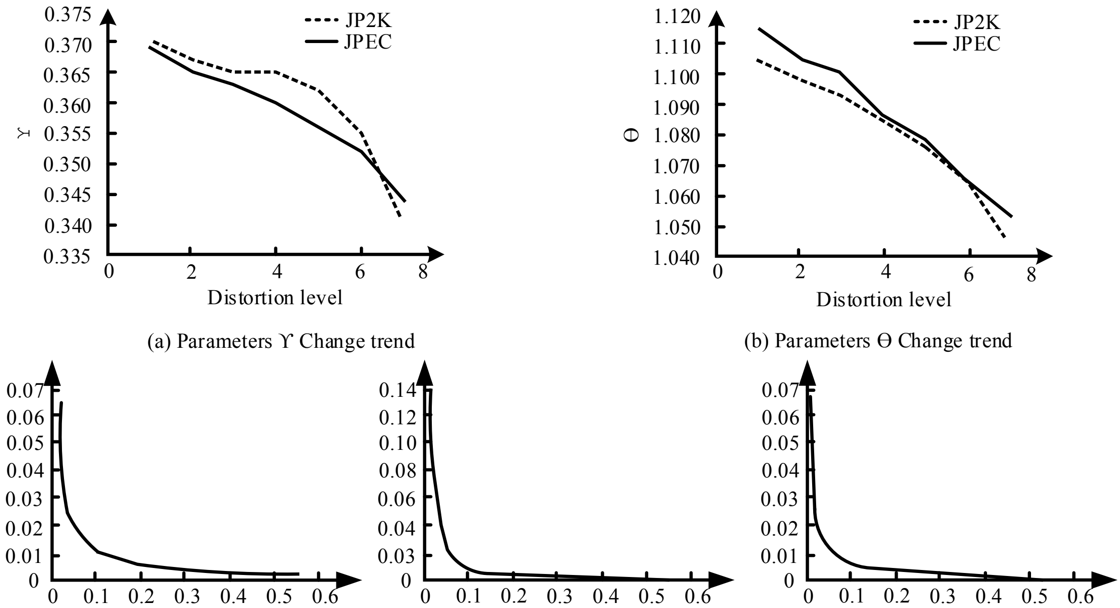

(a) Parameters Υ Change trend

(b) Parameters Θ Change trend

(c) Reference image KLD = 0.0077

(d) JPEG image distortion level = 5 KLD = 0.0036 DMOS = 50.89

(e) Jp2k image distortion level = 4 KLD = 0.0227 DMOS = 52.89

Figure 8 Comparison of performance indexes under different distorted image types

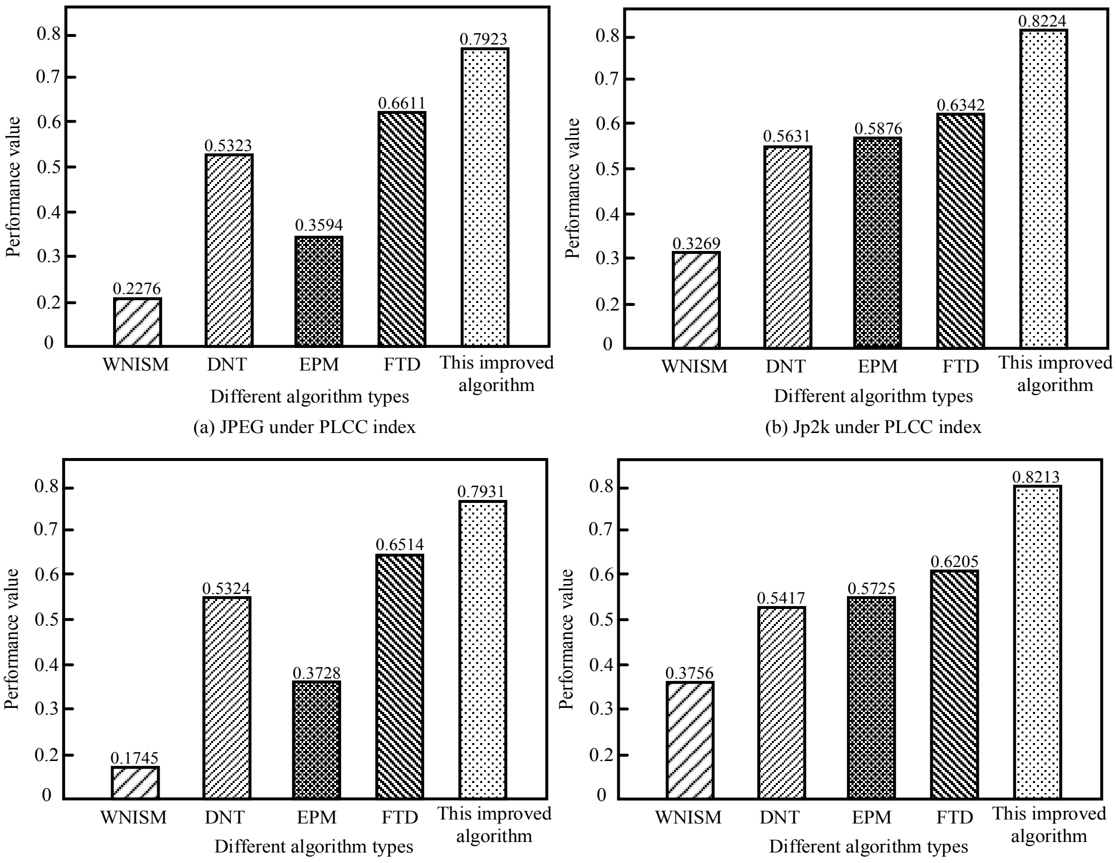

(a) JPEG under PLCC index (b) Jp2k under PLCC index (c) JPEG under SRCC index (d) Jp2k under SRCC index

As can be seen from Figure 8, among the performance values of JPEG distortion type under PLCC index, the highest value is the improved algorithm, the value is 0.7923, the lowest value is WNISM, and the value is 0.2276. Among the three algorithms, FTD with performance value of 0.6611, DNT with performance value of 0.5323 and EPM with performance value of 0.3594 are in turn; among the performance values of jp2k distortion type under PLCC index, the highest value is the improved algorithm, with a value of 0.8224, the lowest value is WNISM and the value is 0.3269. The three algorithms are FTD with a performance value of 0.6342, EPM with a performance value of 0.5876 and DNT with a performance value of 0.5631; among the performance values of JPEG distortion type under SRCC index, the highest value is the improved algorithm, with a value of 0.7931, the lowest value is WNISM and the value is 0.1745. The three algorithms are FTD with a performance value of 0.6514, DNT with a performance value of 0.5324 and EPM with a performance value of 0.3728; under the SRCC index, the highest performance value of jp2k distortion type is the improved algorithm, with a value of 0.8213, the lowest value is WNISM and a value of 0.3756. The three algorithms are FTD with a performance value of 0.6205, DNT with a performance value of 0.5725 and EPM with a performance value of 0.5417. It can be seen that in the comparison of five partial reference quality evaluation algorithms under two different indicators and two different distorted image types, the computational performance value of this study has always been the highest, that is, the performance is the strongest. Comparing the performance values of the improved algorithm with different distorted image types in different performance indexes, it can be seen that the performance value of jp2k distorted image type under PLCC index is the highest, which is 0.8224. It can be seen that the algorithm has the best performance among jp2k distorted image types under PLCC index. The performance value of JPEG distorted image type under PLCC index is the lowest, which is 0.7923. It can be seen that the performance of this algorithm is the worst among JPEG distorted image types under SRCC index. Under the same distorted image type, the performance values of the improved algorithm are relatively similar. Under the JPEG distorted image type, the performance values of the improved algorithm in PLCC index and SRCC index type are relatively similar. The algorithm value of PLCC is 0.7923, while the algorithm value of SRCC is 0.7931, with a difference of only 0.0008. Under the jp2k distorted image type, the performance values of the improved algorithm in PLCC index and SRCC index type are relatively similar. The algorithm value of PLCC is 0.8224, while the algorithm value of SRCC is 0.8213, with a difference of only 0.0009. The difference between two different distortion types of images under the same algorithm performance index is relatively large. Under the JPEG distorted image type, the digital performance value of the improved algorithm under the PLCC detection index is 0.7929, while the digital performance value under the PLCC detection index is 0.8224, with a difference of 0.295. Under the jp2k distorted image type, the digital performance value of the improved algorithm under the PLCC detection index is 0.7931, while the digital performance value under the PLCC detection index is 0.8231, with a difference of 0.03. From the difference values of 0.0295 and 0.03, respectively, it can be seen that the type of distorted image has a great impact on the improved algorithm and the change of measurement indicators in different dimensions cannot affect the performance of the improved algorithm.

3.2 Experimental results and analysis of non-reference quality evaluation for network shared image quality

The non-reference quality evaluation of network shared image quality is also carried out through performance index comparison. The research database mainly consists of the screen content of the network full video. The database contains 11 original video sequences. The average frame rate of the video is 30fps, and the duration is more than 10 s. The distortion types include AVC, HEVC and SCC. This part of the test will be divided into two parts. The first part is aimed at the performance difference of the improved algorithm in PLCC, SRCC and RMSE under different distortion types. PLCC and SRCC are the same as the previous section. The RMSE Index added this time also evaluates the prediction accuracy by performing the nonlinear mapping between subjective and objective scores, the lower the value, the better the performance of the algorithm. The second part evaluates the non-reference quality evaluation algorithm and some reference quality evaluation algorithms under the same index, so as to compare the impact of the amount of reference data on the performance of network shared image quality evaluation algorithm. The image distortion types include AVC, HEVC and SCC. The comparison between different distortion types is shown in Figure 9.

It can be seen from Figure 9 that the PLCC performance value of AVC type is the highest among the three distorted image types in the improved algorithm, and the value is 0.558. The other two are SCC type performance value of 0.479, HEVC type performance value of 0.459, from large to small, AVC, SCC and HEVC, respectively. The PLCC performance value obtained by combining the three distortion pattern types is 0.458. It can be seen that among the three different distortion image types, the performance of the improved algorithm is the best in the AVC type, and the performance is the worst after the synthesis of the three distortion types. Because the image structure synthesised by the three distortion types is the most complex, the effect is within the predictable range. The SRCC performance value of SCC type is the highest among the three distorted image types, and the value is 0.335. The other two types are HEVC type performance value of 0.311 and AVC type performance value of 0.308, from large to small, SCC, HEVC and AVC, respectively. The SRCC performance value obtained by combining the three distortion pattern types is 0.278. It can be seen that among the three different distortion image types, the performance of the improved algorithm in SCC type is the best and the performance after the synthesis of the three distortion types is the worst. Similarly, the image structure synthesised by the three distortion types is the most complex, so the effect is within the predictable range. According to the fitting curves of the three distorted image types, the improved algorithm has better fitting sensitivity to human eyes in the three distorted image types, and the fitting effect of AVG type is the best. It can be seen that the improved non reference quality evaluation algorithm has good consistency with the human visual system, which can effectively reflect the visual effect differences between different distorted image types, and then evaluate the quality of network shared images. The comparison between the performance values of the second part of the algorithm is shown in Figure 10.

Figure 9 Comparison of performance indexes and parameter changes under different distorted image types

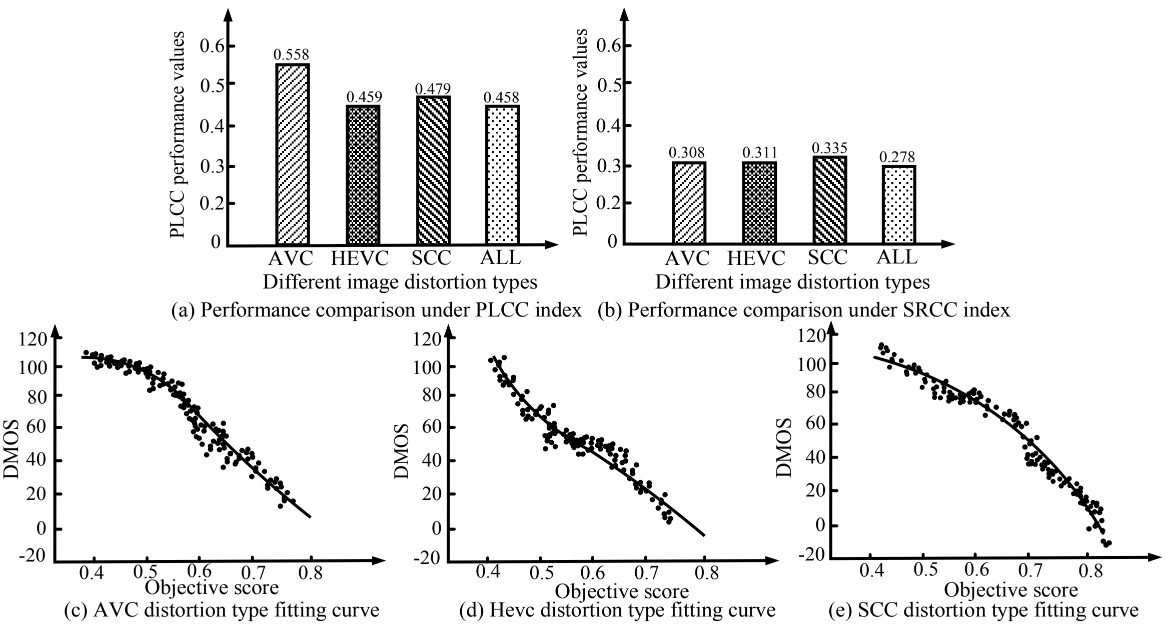

Figure 10 Comparison of performance indexes

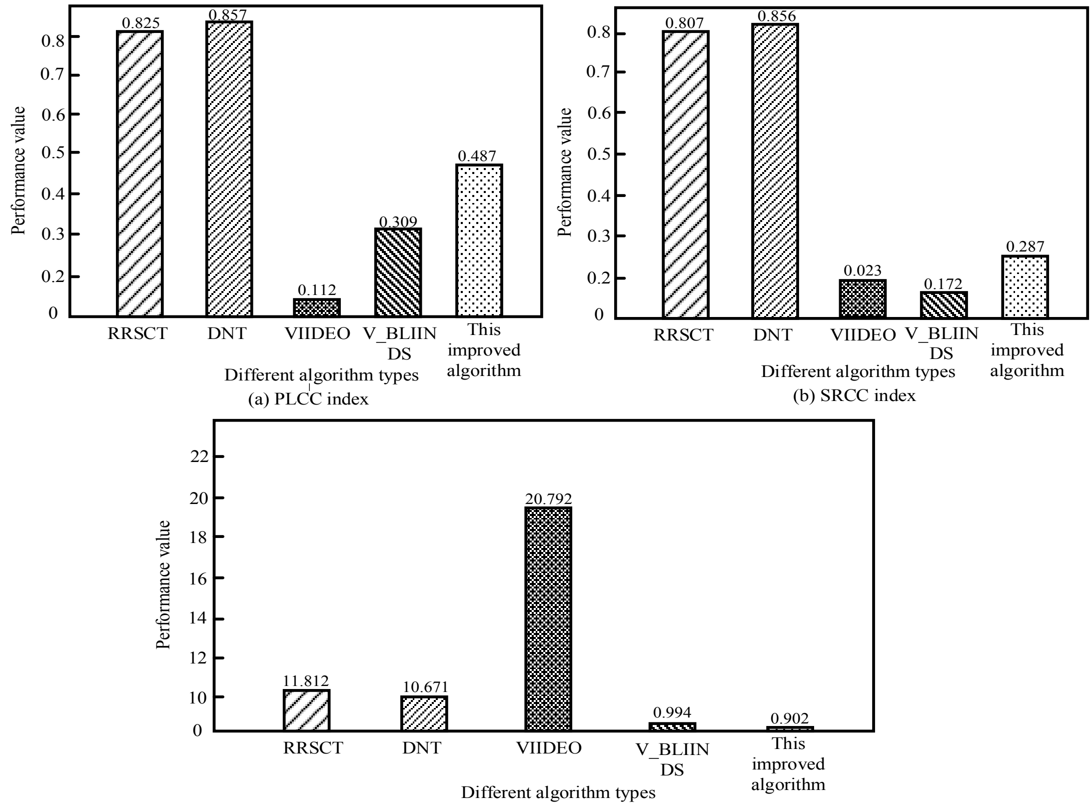

As shown in Figure 10, the four algorithms used for comparison this time are RRSCT, DNT, viideo and V_Bliinds, in which RRSCT and DNT are some reference quality evaluation algorithms, while viideo and V_Bliinds is a non-reference quality evaluation algorithm. In the comparison of PLCC performance indicators, the performance values of the two partial reference quality evaluation algorithms are higher, RRSCT and DNT are 0.825 and 0.857, respectively, while the performance values of no reference quality evaluation algorithm are lower, viideo and V_Bliinds are 0.112 and 0.309, respectively, while the performance of the improved algorithm is 0.487. Among the non-reference quality evaluation algorithms, the improved algorithm has the highest performance and the strongest performance. The performance value of some reference quality evaluation algorithms is relatively low. It can be seen that the number of reference data on PLCC index has a very significant impact on the performance of quality evaluation algorithms; On the SRCC index, the performance values of the two partial reference quality evaluation algorithms are also high, RRSCT and DNT are 0.807 and 0.856, respectively, while the performance values of the non-reference quality evaluation algorithm are low, viideo and V_Bliinds are 0.023 and 0.172, respectively, while the performance of the improved algorithm is 0.287. Among the non-reference quality evaluation algorithms, the improved algorithm has the highest performance and the strongest performance. However, when comparing some reference quality evaluation algorithms, the performance value is low. It can be seen that the number of reference data on SRCC index also has a very significant impact on the performance of quality evaluation algorithm; In the RMSE index, the performance values of the two partial reference quality evaluation algorithms are also high, but not the highest. The highest value appears in the performance value of the non-reference quality evaluation algorithm viideo, which is 20.792, followed by RRSCT and DNT, which are 11.812 and 10.671, respectively, while the non-reference quality evaluation algorithm v_ The performance value of bliinds is 0.994. The lowest performance value appears in the improved quality evaluation algorithm, and the performance value is 0.902. Because the smaller the performance value of RMSE index, the better the performance is, so the improved quality evaluation algorithm is the algorithm with the best performance in RMSE index. And the influence of the reference data of RMSE index on the performance of quality evaluation algorithm is not significant. To sum up, some of the improved reference quality evaluation algorithms and no reference quality evaluation algorithms show excellent performance in the same type of algorithms, and perform better in different distorted image types. The experimental results also prove that the number of statistical parameters can have a great impact on the performance of quality evaluation algorithm.

4 Conclusion

With the development of computer and network technology, network image and video sharing have become one of the indispensable means of work and entertainment and the distortion quality of computer network shared image significantly affects the user experience. This study analyses the sensitive characteristics of human visual system, classifies and optimises the computer network shared image distortion quality evaluation system based on human visual perception of image quality, and puts forward improved algorithms from two parts: partial reference image quality evaluation and non-reference image quality evaluation. In the part of reference image quality evaluation, the algorithm is improved on the image content features and visual sensitive features, while in the part of non-reference image quality evaluation, combined with the characteristics of human vision, the algorithm is improved from the two parts of time features and spatial features. Then, the new energy of the two improved algorithms is analysed by comparative experiments. The results show that in the part of reference image quality evaluation, the performance values of JPEG and jp2k image distortion types are the maximum in PLCC index, which are 0.7923 and 0.3224. On the SRCC index, the performance values of JPEG and jp2k image distortion types are also the maximum, which are 0.7931 and 0.8213; In the non-reference image quality evaluation part, the improved algorithm has good fitting effect under SCC, HEVC and AVC3 distortion types, and the performance values on PLCC and SRCC indexes are the highest values in the non-reference image quality evaluation algorithm, which are 0.487 and 0.287, respectively. On the RMSE index, the value is the lowest value, which is 0.902. In quality evaluation of some reference images, it is found that the PLCC and SRCC values of some reference image quality evaluation algorithms are generally higher. It can be seen that the number of statistical parameters can have a great impact on the performance of the quality evaluation algorithm. However, the non-reference images/imaged quality evaluation algorithm has lower values of the RMSE index, does not need reference data, and has a wider application range and stronger robustness. Computational efficiency is also higher. In conclusion, the improved algorithm fully shows its own performance advantages in the comparative test, is more suitable for the evaluation of image distortion quality shared by computer network, has higher calculation efficiency and has wider application prospects.

References

Aich, S., Stavness, I. and Taniguchi, Y. et al. (2020) 'Multi-scale weight sharing network for image recognition', *International Journal of Pattern Recognition Letters*, Vol. 131, pp.348–354.

Akb, A., Ak, B. and Akb, B. et al. (2019) 'Script identification in natural scene image and video frames using an attention based convolutional-LSTM network – ScienceDirect' *International Journal of IEEE Sensors Journal*, Vol. 85, pp.172–184.

Bouida, A., Khelifi, M. and Beladgham, M. et al. (2021) 'Monte Carlo optimization of a combined image quality assessment for compressed images evaluation', *International Journal of Traitement du Signal*, Vol. 38, No. 2, pp.81–289.

Chen, Z., Zhang, S. and Zhang, J. et al. (2021) 'A novel artificial intelligence model for color image quality assessment for security enhanement weighted by visual saliency', *International Journal of Intelligent and Fuzzy Systems*, Vol. 40, No. 4, pp.8091–8100.

Fang, Z., Wang, X. and Ji, W. et al. (2021) 'geometric calibration and image quality assessment of high resolution dual-camera satellite', *International Journal of Beijing Institute of Technology*, Vol. 30, No. 2, pp.125–138.

Lei, Y. (2022) 'Research on microvideo character perception and recognition based on target detection technology', *International Journal of Computational and Cognitive Engineering*, Vol. 1, No. 2, pp.83–87.

Meng, C., An, P. and Huang, X. et al. (2020) 'Full reference light field image quality evaluation based on angular-spatial characteristic', *International Journal of IEEE Signal Processing Letters*, Vol. 27, No. 99, pp.525–529.

Ng, S., Wolkow, R. and Walus, K. et al. (2020) 'A design and simulation tool for atomic silicon quantum dot circuits', *International Journal of IEEE Transactions on Nanotechnology*, Vol. 19, No. 99, pp.137–146.

Qu, Q., Chen, X. and Chung, V. et al. (2021) 'Light field image quality assessment with auxiliary learning based on depthwise and anglewise separable convolutions', *International Journal of IEEE Transactions on Broadcasting*, Vol. 99, pp.1–14.

Song, C., Zeng, P. and Wang, Z. et al. (2019) 'Image forgery detection based on motion blur estimated using convolutional neural network', *International Journal of IEEE Sensors Journal*, Vol. 19, No. 23, pp.348–354.

Wang, C., Zhang, M. and Su, Z. et al. (2019a) 'ILearning a multi-level guided residual network for single image deraining', *International Journal of Signal Processing: Image Communication*, Vol. 78, pp.206–215.

Wang, X., Liang, X. and Yang. B. et al. (2019b) 'No-reference synthetic image quality assessment with convolutional neural network and local image saliency', *International Journal of Computational Visual Media*, Vol. 5, No. 2, pp.193–208.

Xiao, J., Liu, T. and Zhao, R. et al. (2021) 'Balanced distortion and perception in single-image super-resolution based on optimal transport in wavelet domain', *International Journal of Neurocomputing*, Vol. 464, pp.408–420.

Yang, Y. and Song, X. (2022) 'Research on face intelligent perception technology integrating deep learning under different illumination intensities', *International Journal of Computational and Cognitive Engineering*, Vol. 1, No. 2, pp.32–36.

Zhaolin, L.U., Zhang, Z. and Wang, Y. et al. (2021) 'SEM image quality assessment based on texture inpainting', *International Journal of IEICE Transactions on Information and Systems*, Vol. E104, No. D(2), pp.341–345.